Supporting information

Red-tunable LuAG Garnet Phosphor via Eu^{3+}→Mn^{4+} Energy Transfer for Optical Thermometry Sensors Application

Bing Yan,[a] Yi Wei,*[,b] Wei Wang,[b] Meiqian Fu,[b] Guogang Li*[,b]

[a] School of Environmental Studies, China University of Geosciences, 388 Lumo Road, Wuhan 430074, P. R. China.

[b] Engineering Research Center of Nano-Geomaterials of Ministry of Education, Faculty of Materials Science and Chemistry, China University of Geosciences, 388 Lumo Road, Wuhan 430074, P. R. China. E-mail: ggli@cug.edu.cn

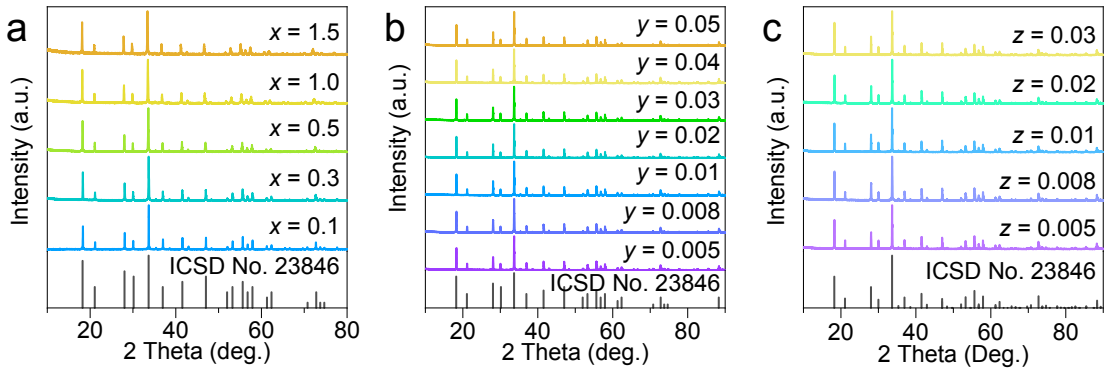

Figure S1. The XRD data of (a) LuAG:$x$$Eu^{3+}$ ($0.1 \le x \le 1.5$), (b) LuAG:$y$$Mn^{4+}$ ($0.005 \le y \le 0.05$) and (c) LuAG:0.05Eu^{3+}, $z$$Mn^{4+}$ ($0.1 \le z \le 1.5$) phosphors, and the standard $Lu_3Al_5O_{12}$ (ICSD No. 23846) is used as a reference.

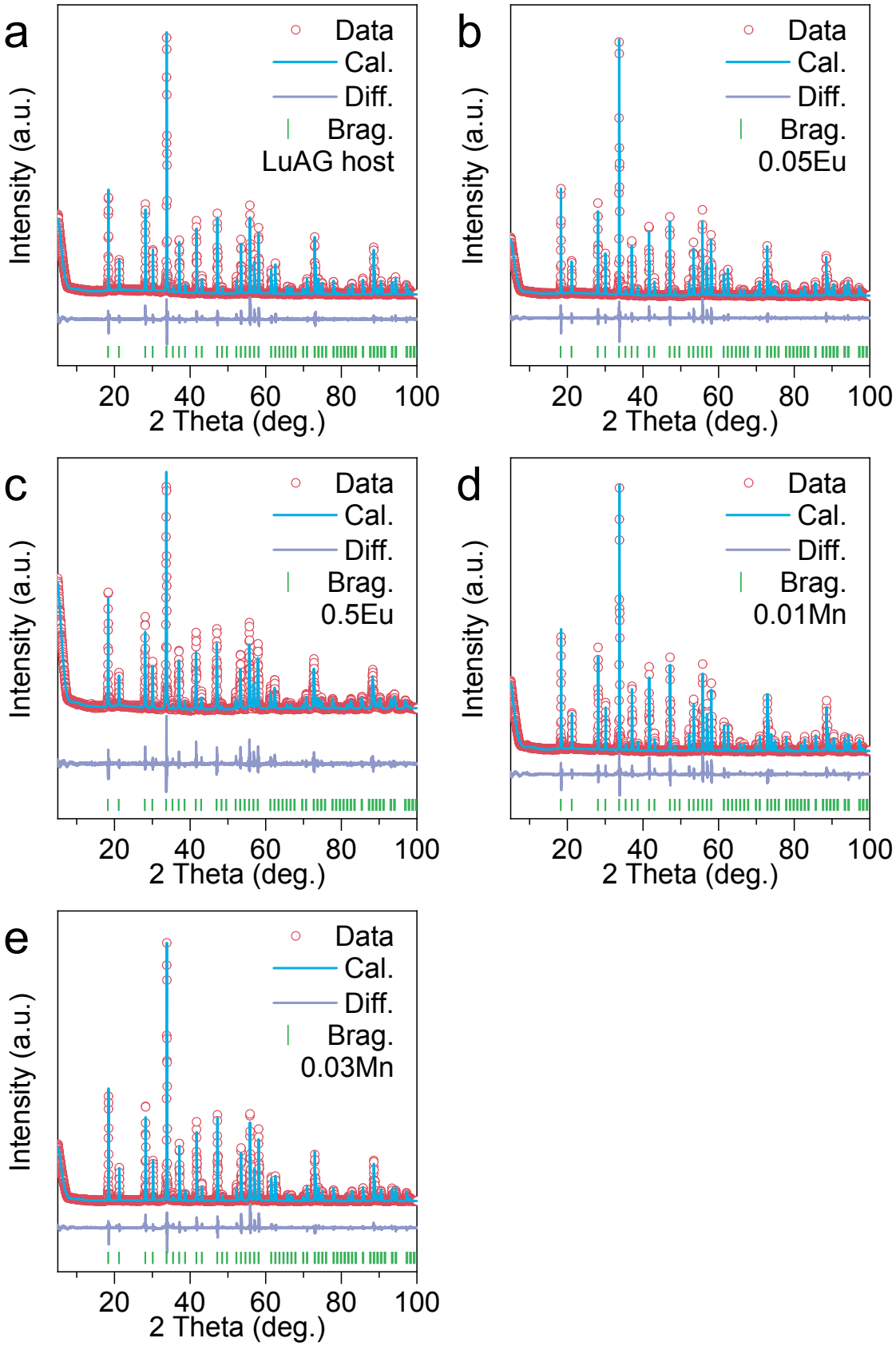

Figure S2. The Rietveld refinement data of (a) LuAG host, (b) LuAG:0.05Eu^{3+}, (c) LuAG:0.5Eu^{3+}, (d) LuAG:0.01Mn^{4+}, and (e) LuAG:0.03Mn^{4+} phosphors.

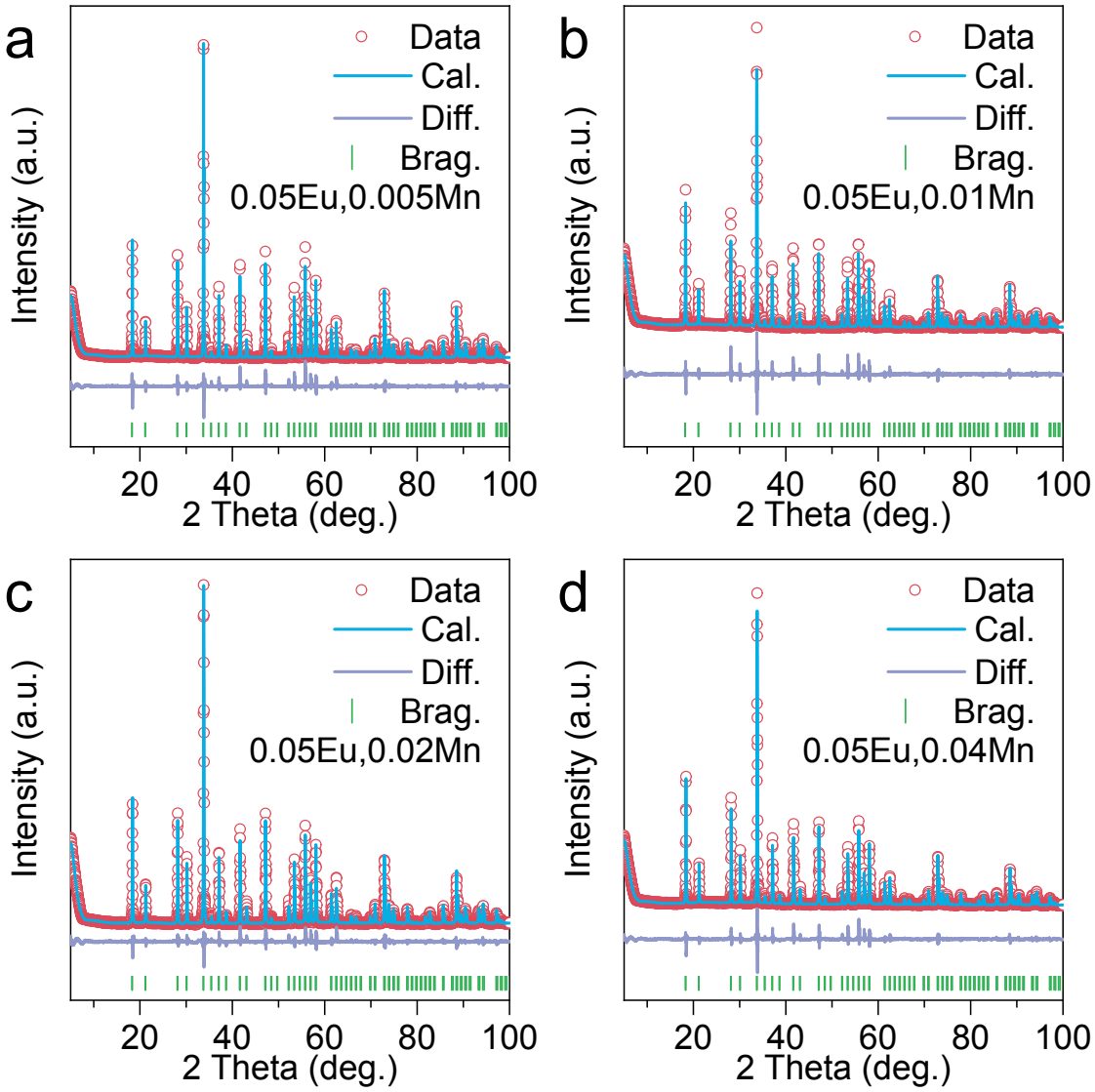

Figure S3. The Rietveld refinement data of (a) LuAG:0.05Eu^{3+}, 0.005Mn^{4+}, (b) LuAG: 0.05Eu^{3+}, 0.01Mn^{4+}, (c) LuAG: 0.05Eu^{3+}, 0.02Mn^{4+}, and (d) LuAG: 0.05Eu^{3+}, 0.04Mn^{4+}.

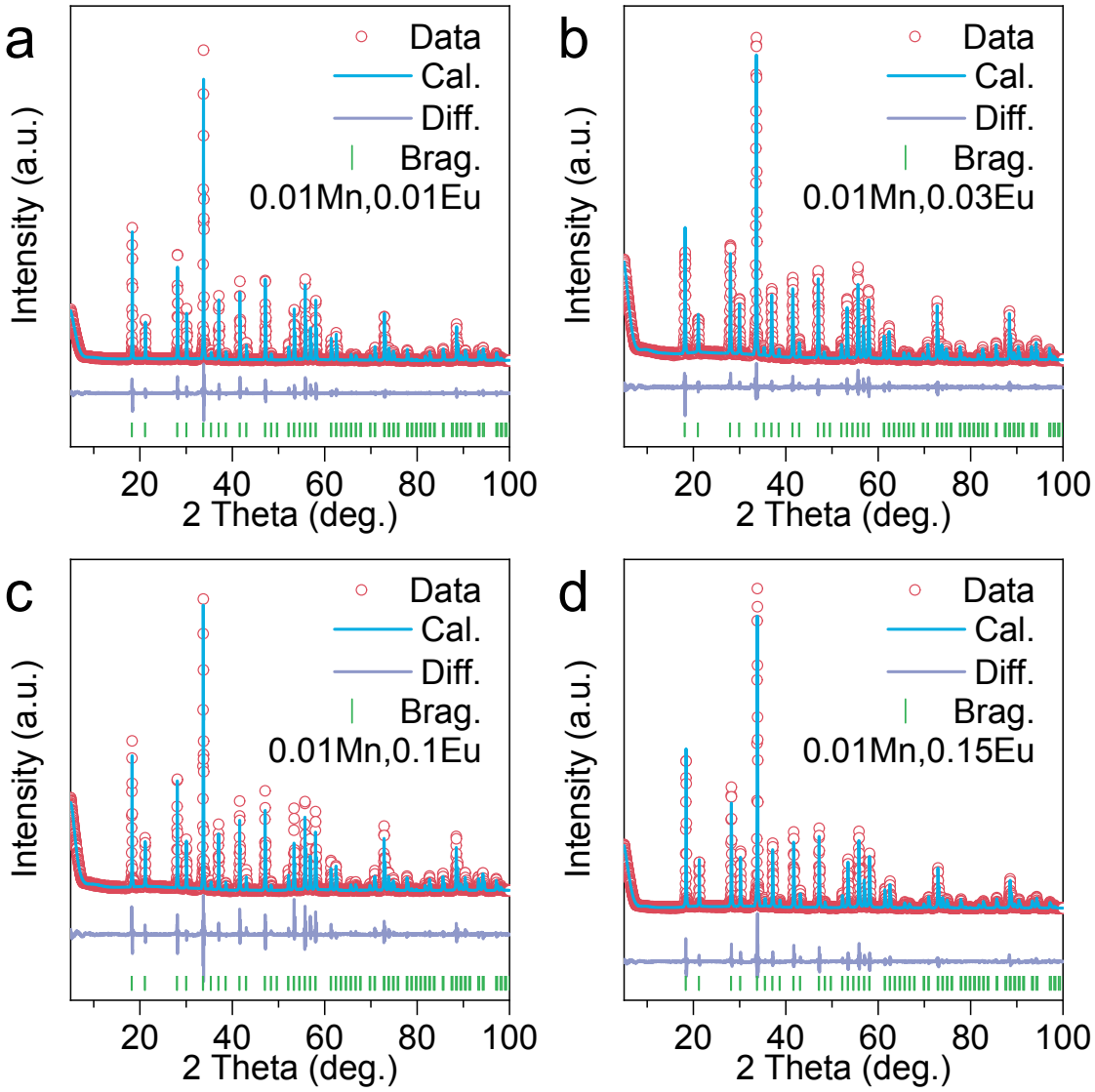

Figure S4. The Rietveld refinement data of (a) LuAG:0.01Mn^{4+}, 0.01Eu^{3+}, (b) LuAG:0.01Mn^{4+}, 0.03Eu^{3+}, (c) LuAG:0.01Mn^{4+}, 0.1Eu^{3+}, and (d) LuAG:0.01Mn^{4+}, 0.15Eu^{3+}.

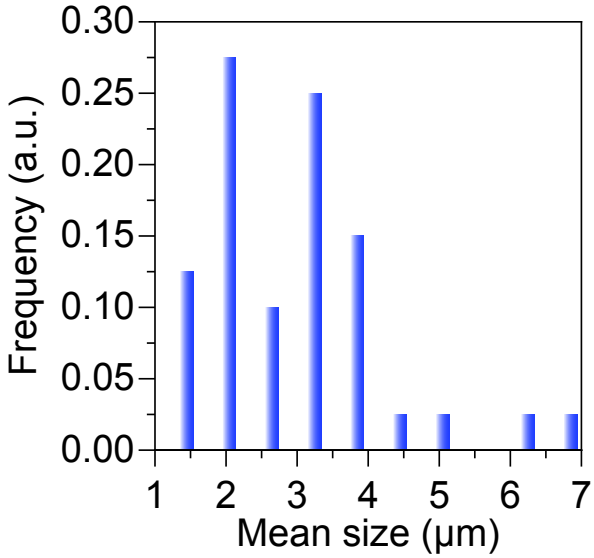

Figure S5. Mean particle size distribution based on SEM image.

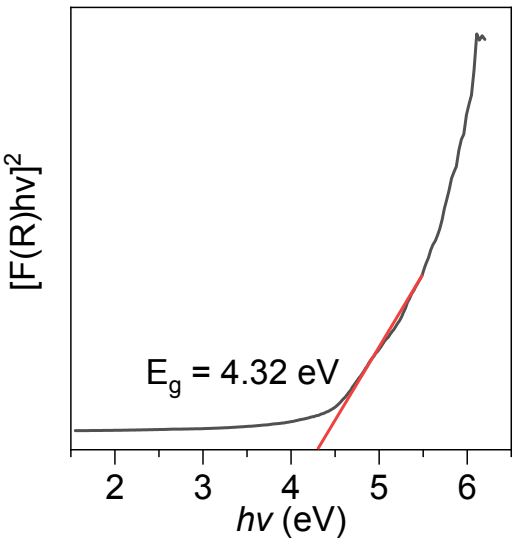

Figure S6. Optical bandgap calculation of LuAG host based on the linear extrapolation.

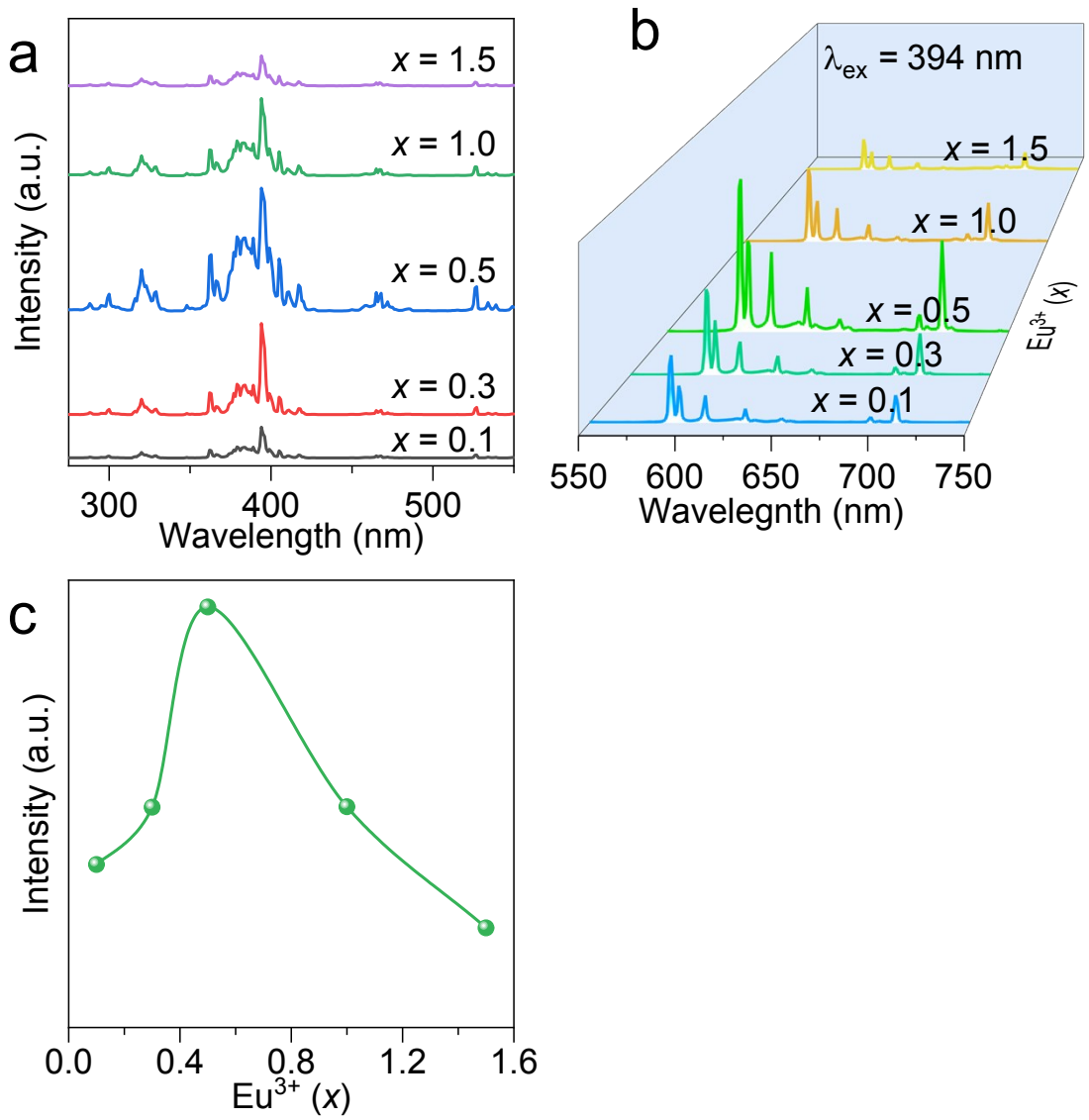

Figure S7. (a) Photoluminescence excitation spectra of LuAG:xEu^{3+} ($0.1 \leq x \leq 1.5$) phosphors under 593 nm excitation. (b) Photoluminescence emission spectra of LuAG:xEu^{3+} ($0.1 \leq x \leq 1.5$) phosphors under 393 nm excitation. (c) The peak intensity of 593 nm as function of Eu^{3+} concentration.

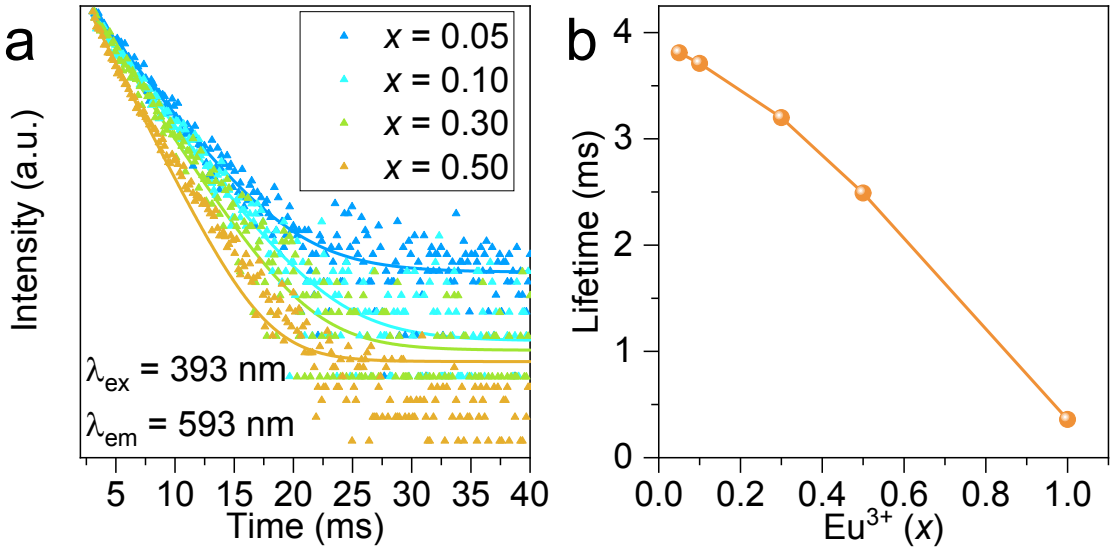

Figure S8. (a) Photoluminescence decay curves of LuAG:xEu^{3+} ($0.05 \leq x \leq 0.5$) phosphors under the excitation of 393 nm and emission of 593 nm. (b) The calculated lifetime values as function of Eu^{3+} doping concentration.

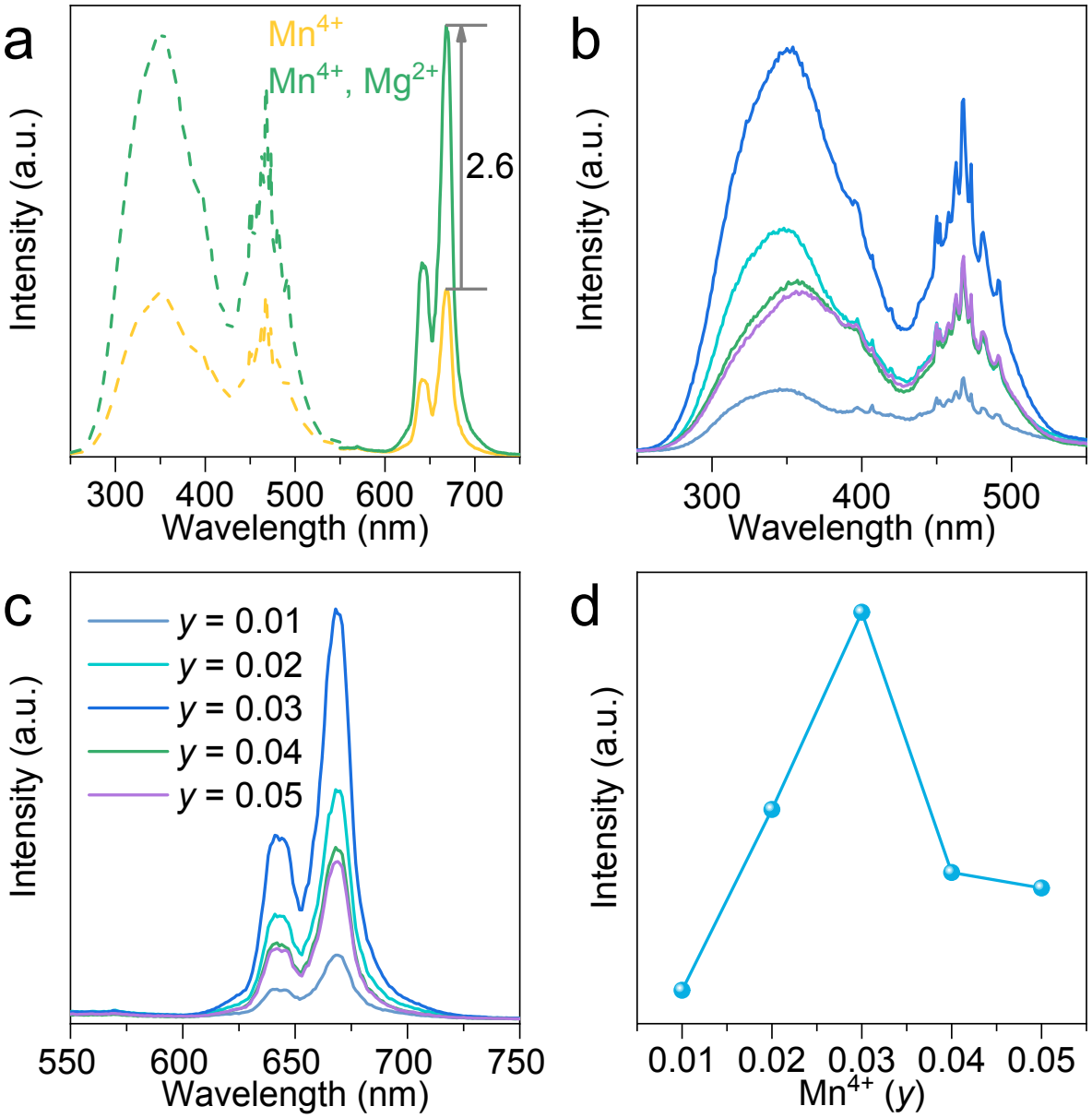

Figure S9. (a) The comparison of PL spectra of LuAG:0.03Mn^{4+} and LuAG:0.03Mn^{4+}, 0.03Mg^{2+} phosphors. (b) Photoluminescence excitation spectra of LuAG:*y*Mn^{4+} ($0.01 \le y \le 0.05$) phosphors under 668 nm excitation. (c) Photoluminescence emission spectra of LuAG:*y*Mn^{4+} ($0.01 \le y \le 0.05$) phosphors under 350 nm excitation. (d) The peak intensity of 668 nm as function of Mn^{4+} concentration.

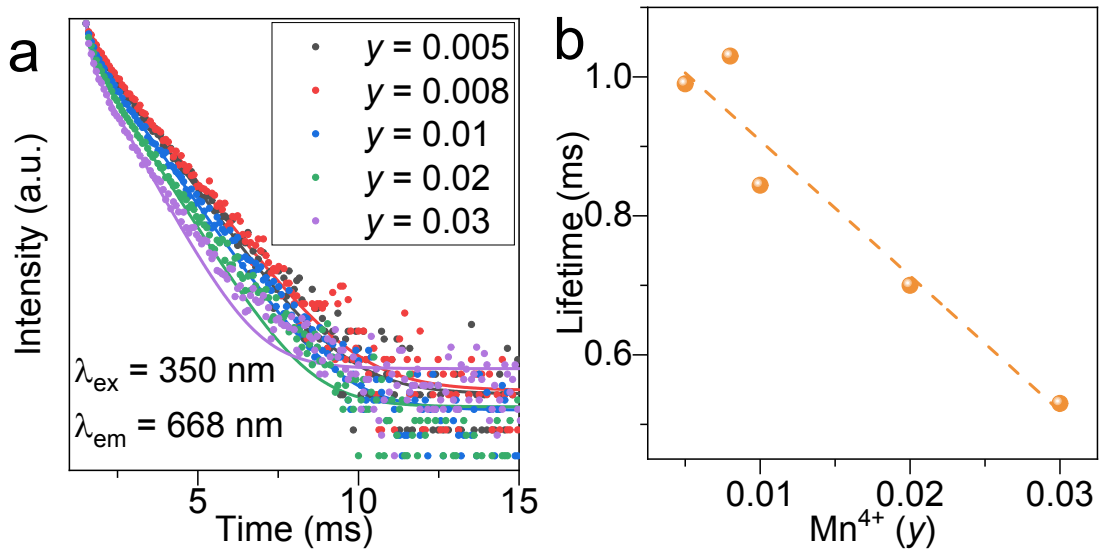

Figure S10. (a) Photoluminescence decay curves of LuAG:yMn^{4+} ($0.005 \leq y \leq 0.03$) phosphors under the excitation of 350 nm and emission of 668 nm. (b) The calculated lifetime values as function of Eu^{3+} doping concentration.

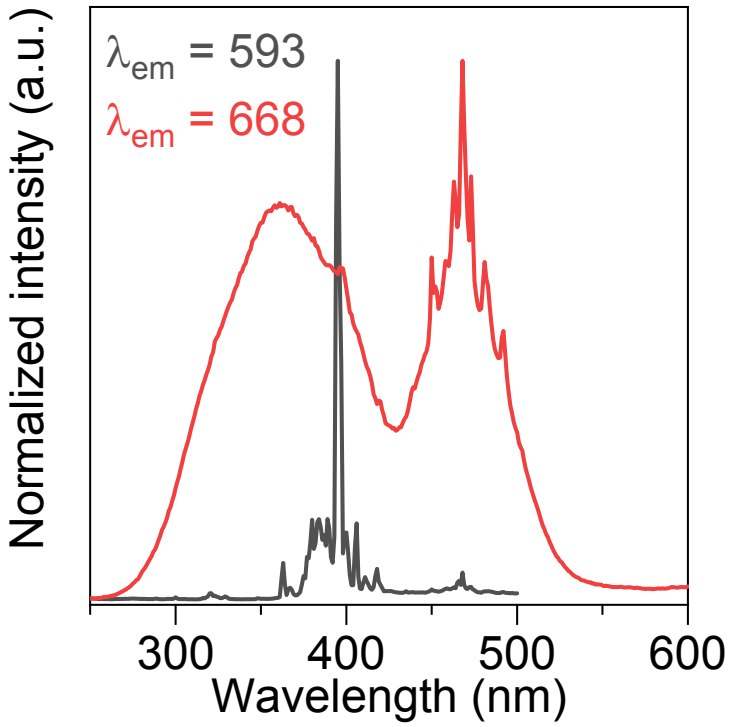

Figure S11. Photoluminescence excitation spectra of LuAG:0.05Eu^{3+}, 0.01Mn^{4+} phosphor under the emission wavelengths of 593 nm and 668 nm.

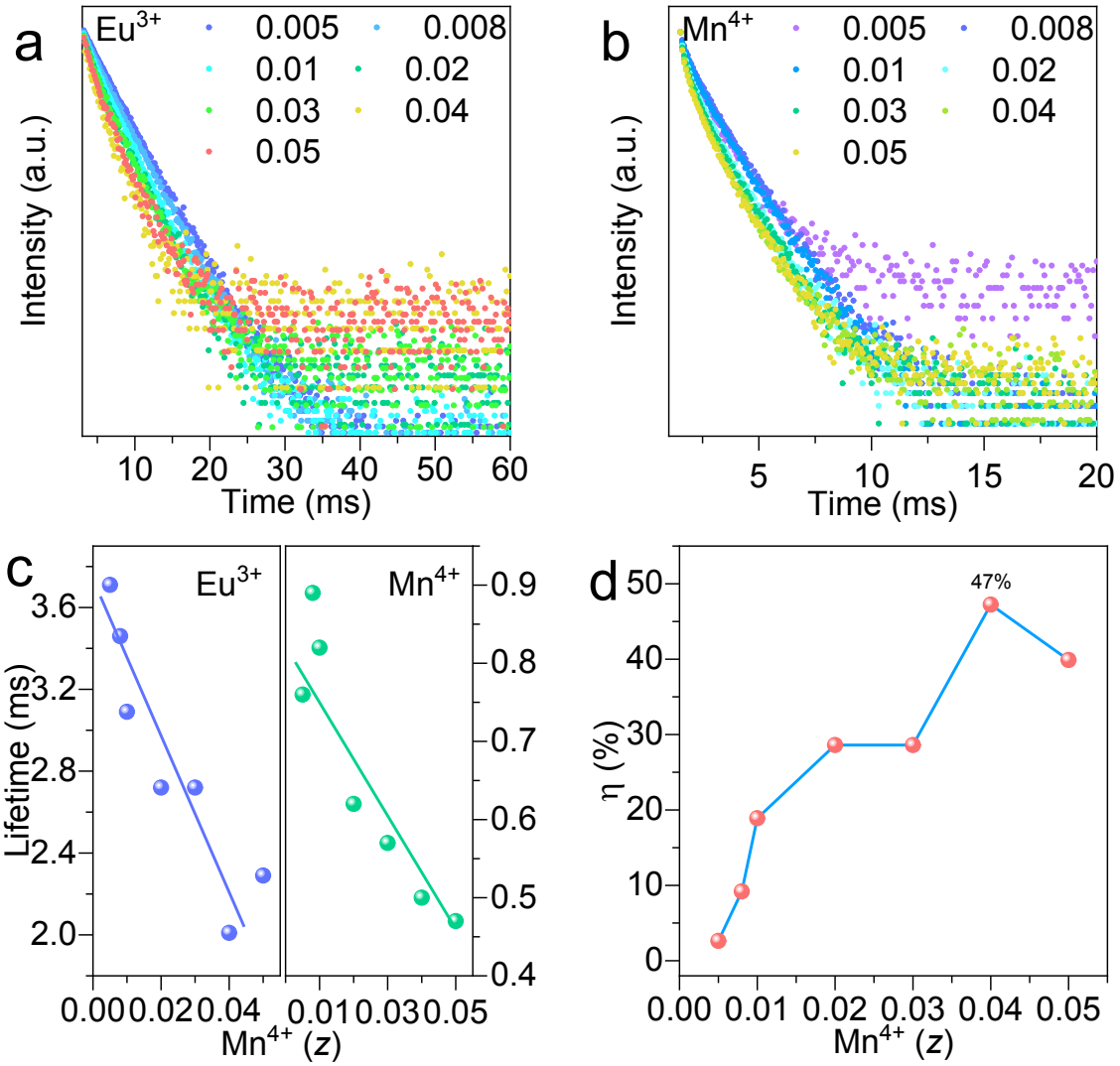

Figure S12. Photoluminescence decay curves of LuAG:0.05Eu^{3+}, zMn^{4+} (0.005 ≤ *y* ≤ 0.05) phosphors (a) under the excitation of 393 nm and emission of 593 nm and (b) under the excitation of 350 nm and emission of 668 nm. (c) The calculated lifetime values of Eu^{3+} and Mn^{4+} peaks as functions of Mn^{4+} doping concentration. (d) Eu^{3+}→Mn^{4+} energy transfer efficiency (η) *vs* Mn^{4+} concentration.

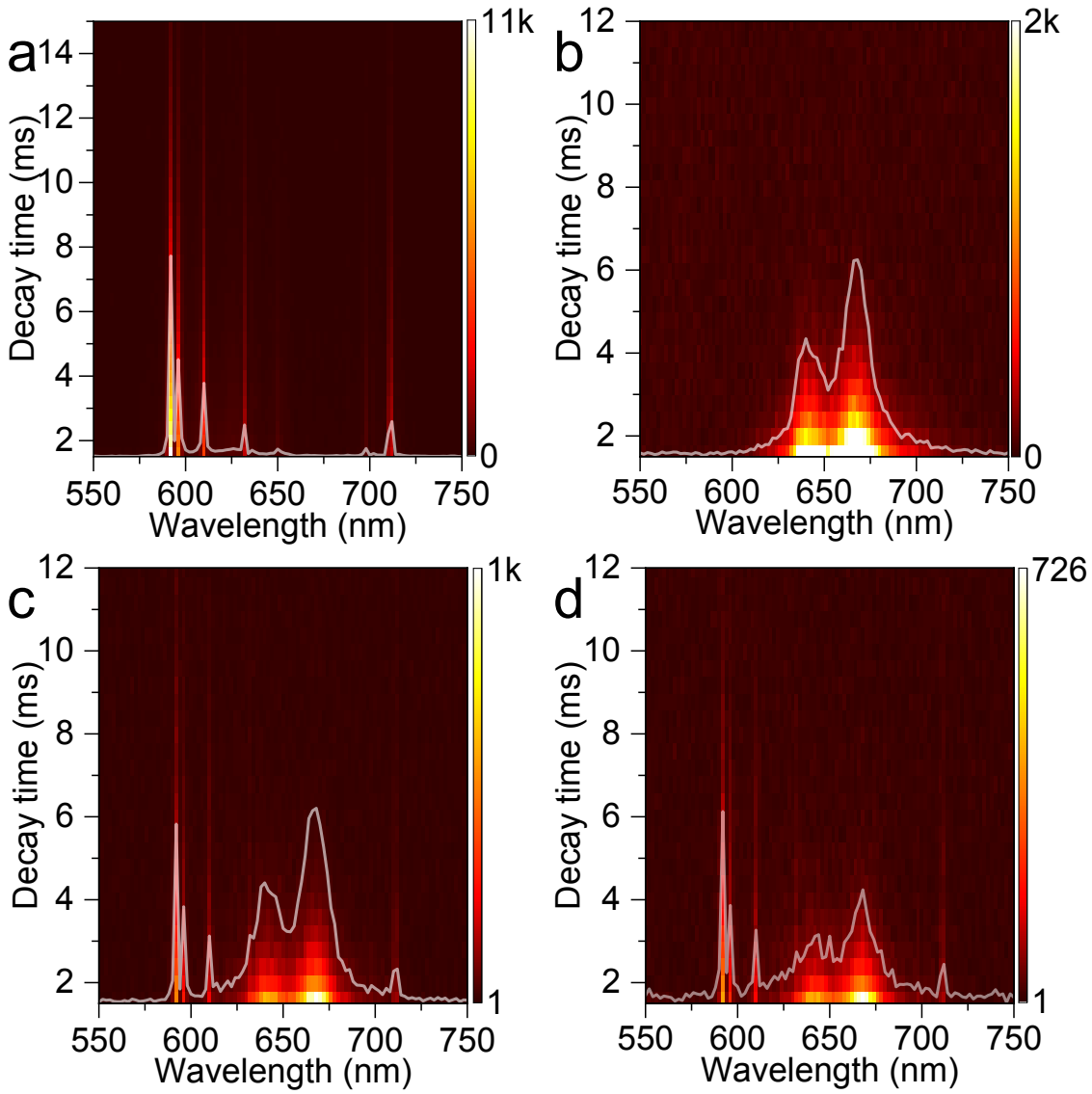

Figure S13. Time-resolved PL spectra and the representative PL spectra of (a) LuAG:0.05Eu^{3+}, (b) LuAG:0.03Mn^{4+}, (c) LuAG:0.05Eu^{3+},0.02Mn^{4+} and (d) LuAG:0.05Eu^{3+},0.03Mn^{4+} phosphors.

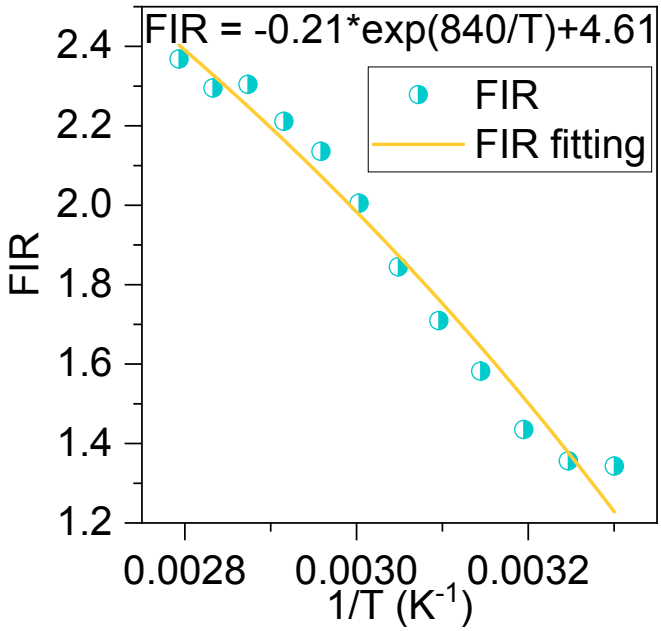

Figure S14. The fitting curve of temperature-dependent FIR(IEu^{3+}/IMn^{4+}) for LuAG:0.05Eu^{3+}, 0.01Mn^{4+} phosphor.